

Flight Testing of Mission Adaptive Compliant Wing

Joel A. Hetrick*, Russell F. Osborn†, Sridhar Kota‡
FlexSys Inc., Ann Arbor, MI, 48105

Peter M. Flick§ and Donald B. Paul**
Air Force Research Laboratory, Dayton, OH, 45433

This paper describes flight test results of a “Mission Adaptive Compliant Wing” (MAC-Wing) variable geometry trailing edge flap in conjunction with a natural laminar flow airfoil. The MAC-Wing technology provides lightweight, low power, variable geometry reshaping of the upper and lower flap surface with no seams or discontinuities. In this particular program, the airfoil-flap system is optimized to maximize the laminar boundary layer extent over a broad lift coefficient range for endurance aircraft applications. The expanded “laminar bucket” capability allows the endurance aircraft to significantly extend their range (15% or more) by continuously optimizing the wing L/D throughout the mission. The wing was tested at full-scale dynamic pressure, full scale Mach, and reduced-scale Reynolds Numbers on Scaled Composites’ White Knight aircraft. Test results confirmed laminar flow regime up to approximately 60% chord for much of the lift range. Analysis and test results suggest significant fuel savings, weight savings and a higher control authority. Preliminary drag results, future aerodynamic applications and vehicle performance projections are discussed.

Nomenclature

A	=	aspect ratio
C_P	=	pressure coefficient
C_L	=	lift coefficient
C_M	=	quarter chord moment coefficient
g_2	=	total pressure in airfoil wake region
g_∞	=	ambient total pressure
M_∞	=	Mach number
p_2	=	static pressure in airfoil wake region
p_∞	=	ambient static pressure
q_∞	=	ambient dynamic pressure
α	=	angle of attack
α'	=	reduced angle of attack due to wing aspect ratio
γ	=	specific heat ratio of air = 1.4

I. Introduction

Working with funding support from Air Force Research Labs (AFRL)’s Air Vehicles Directorate, FlexSys Inc. has developed a unique, variable-geometry, trailing edge flap that can re-contour the airfoil upper and lower surface¹. Since the weight of long endurance aircraft can vary by fifty percent or more over the course of a mission, the ability to minimize drag across a wide operating lift coefficient range provides a significant performance increment for any aircraft that incorporates the compliant flap technology. FlexSys has applied the compliant flap system to an aggressive Natural Laminar Flow (NLF) airfoil developed for SensorCraft² applications. This airfoil can theoretically achieve up to 65% chord laminar flow on the upper surface and up to 90% chord laminar flow on the lower surface. Because NLF airfoils with long laminar runs have steep pressure gradients in the pressure

* Vice President, FlexSys Inc., email: hetrick@flxsys.com

† Aero Specialist, FlexSys Inc., email: osbornrf@flxsys.com

‡ President, FlexSys Inc., email: kota@flxsys.com

§ Program Manager, AFRL – Air Vehicles Directorate, email: Peter.Flick@wpafb.af.mil

** Chief Scientist, AFRL – Air Vehicles Directorate, email: Donald.Paul@wpafb.af.mil

recovery region, the gentle curvature change provided by a compliant flap can reduce or eliminate flow separation over the flap surface as opposed to a rotational flap which can introduce flow separation at the flap knee. Analyses and flight test results indicate that long laminar runs and low drag can be maintained while the compliant trailing edge flap is significantly deflected.

A. Mission Adaptive Compliant Wing Technology

In contrast to conventional elastic mechanisms that employ flexible hinges, the Mission Adaptive Compliant Wing (MAC-Wing) wing uses sophisticated algorithms to design the topology and shape of an internal structure that deforms as a whole rather than concentrating the flexion in localized regions and avoiding high-stress concentrations. This design paradigm of *distributed* compliance offers additional benefits since the whole adaptive structure is viewed as a compliant mechanism¹ that can move into complex predetermined positions with only minimal force and can be locked in place at any desired configuration. While these structures have been described as “flexible”, they are optimized to resist deflection under significant external aerodynamic loading and are actually quite stiff and strong. The elimination of discontinuities in the flap surface can provide lower drag and higher control authority than comparable hinged flaps. Furthermore, the elimination of joints and seams can provide a signature reduction while also making the flap more impervious to icing and fouling due to debris.

While the current research focuses on a trailing edge adaptive structure, FlexSys has developed morphing surfaces for both the leading and trailing edge; and for both fixed wing and rotorcraft applications. Research is targeted at minimizing the force required to morph surfaces while maintaining maximum stiffness to withstand external loading. Design and optimization algorithms account for external (air) loads, actuator force and displacement, morphing shape error, overall system weight, buckling forces and package constraints in addition to overall system complexity and material fatigue. A few design iterations are generally required to resolve conflicting design requirements between aeroelastic behavior and the compliant structure design. Several models have been built and tested to measure aerodynamic and structural performance.

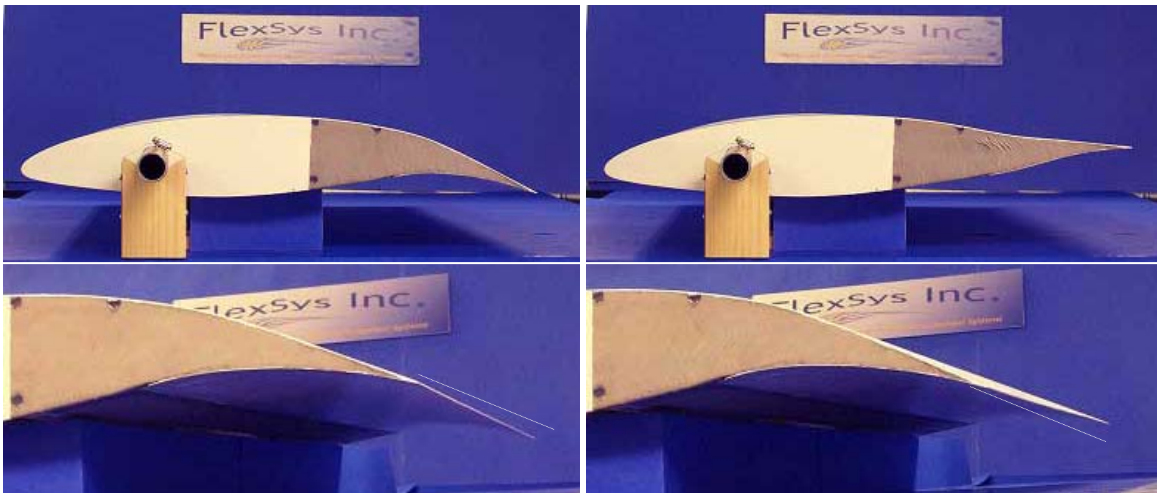


Figure 1. Flexsys Inc.’s Mission Adaptive Compliant Wing trailing edge designed for a high altitude long endurance aircraft undergoing +/- 10-degree flap deflection with a 3-degree twist. The airfoil and the morphing flap combination were designed to support an aggressive, 65% laminar boundary layer (chord-wise) on the upper surface.

In order to produce motion, a MAC-Wing flap must elastically strain the underlying flap structure. The required energy to re-shape the structure is minimized during optimization. Even with the additional force required to elastically deform the structure, these flaps work against the aerodynamic loading differently than a hinged flap. Comparing the peak power draw during a high rate movement, MAC-Wing flaps can actually require less force and less power than a comparably sized conventional flap. One study comparing a MAC-Wing flap to a conventional trailing edge flap during a max G pull-up maneuver showed that the MAC-Wing flap actually required 33% less actuation force and 17% lower peak actuation power.

The aerodynamic benefits of a smooth, variable camber flap are significant. Comparing equally sized trailing edge flaps, MAC-Wing flaps can provide up to a 40% increase in control authority per degree deflection over hinged control surfaces. These gains can be realized with up to 25% lower drag. The boost in aerodynamic performance

occurs not only at the aft portion where the trailing edge is located, but over the entire airfoil chord. Forward of the trailing edge, the increased performance is a result of increased circulation and elevated leading edge suction (stagnation point control) created by the variable geometry technology. Figure 2 (a) illustrates aerodynamic analysis of a MAC-Wing trailing edge flap performed using XFOIL. Note that laminar flow is maintained for a longer chord percentage for the MAC-Wing flap as compared to the conventional (pure rotating) flap. Figure 2 (b) illustrates a direct comparison of the conventional flap L/D performance compared to the MAC-Wing flap L/D performance. In some cases the MAC-Wing flap achieves nearly a 75% increase in L/D.

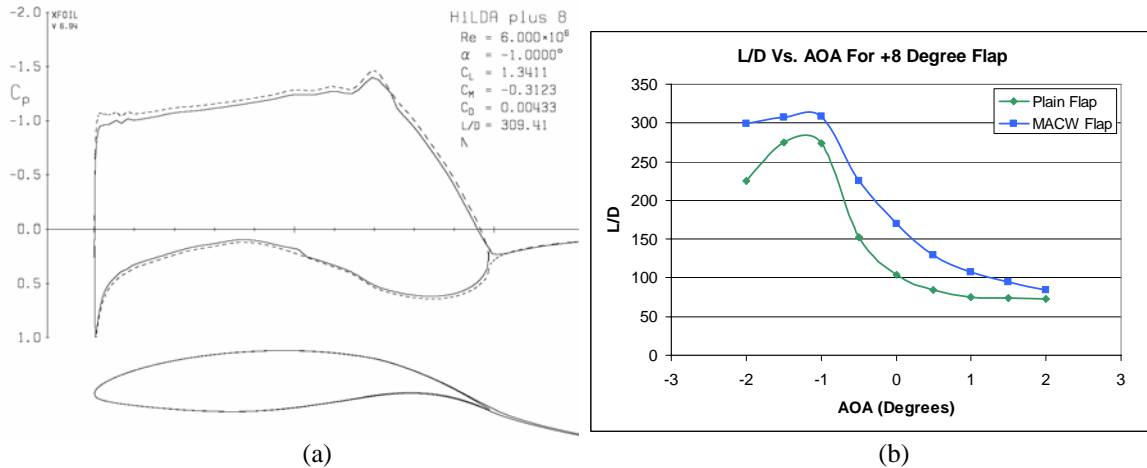


Figure 2. (a) XFOIL analysis of a plain flap with a +8 degree flap deflection. (b) XFOIL analysis showing L/D comparison of a plain flap and a MAC-Wing flap at +8 degree flap deflection.

To date, MAC-Wing prototypes have been fabricated from aircraft grade aluminum. These structures are estimated to weigh roughly 30% more than an all-up composite, sandwich-structure conventional flap. Progression to a full composite MAC-Wing flap is underway and is estimated to provide significant reductions in weight (20% to 30% weight reduction) as well as gains in strength and allowable deflection range.

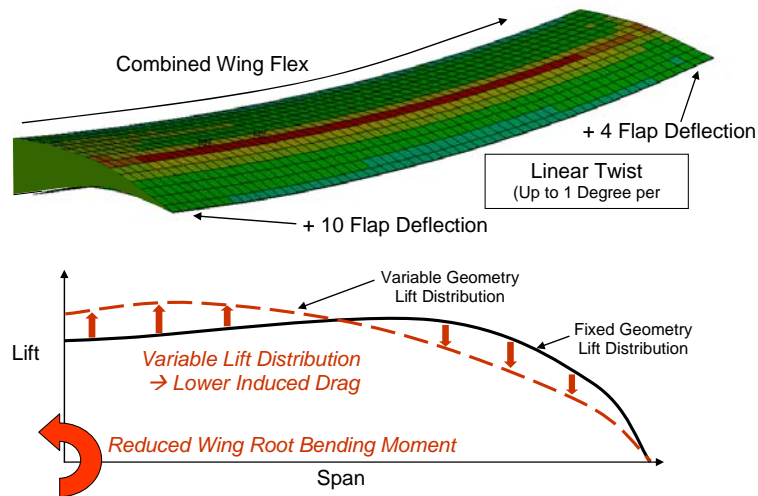


Figure 3. Capability of the MAC-Wing control surfaces to produce differential deflection along the span of a wing thereby providing spanwise load tailoring for wing root bending moment control and lift distribution control resulting significant weight savings.

Finally, MAC-Wing technology allows the flap to be positioned with a linearly varying flap deflection along the wing span. Extensive simulation under aerodynamic loading, wing flex, and flap twist (Figure 3) illustrate that these structures can safely withstand these multitude of loads while keeping material strains within their cyclic limits. This differential deflection capability allows a vehicle equipped with MAC-Wing flaps to create subtle adjustments

to the spanwise lift distribution. This has the benefit of allowing the flap to reshape the wing lift distribution closer to an elliptical distribution, minimizing induced drag, and/or by reducing the lift levels on outboard sections of the wing in order to minimize the wing root bending moment – thus potentially saving weight.

B. High-Altitude Long Endurance “SensorCraft” Application

The U.S. Air Force Research Laboratory (AFRL) has identified certain feasible vehicle concepts and aerodynamic technology development requirements for a high-altitude long-endurance intelligence-surveillance-reconnaissance (ISR) concept vehicle known as SensorCraft². SensorCraft is conceived as an unmanned air vehicle system performing command, control, detection, identification, tracking, relay, and targeting functions for long durations at extended ranges. It is the air-breather component of a fully integrated intelligence, surveillance, and reconnaissance (ISR) enterprise that incorporates air, space, and ground components.

MAC-Wing adaptive structures technology allows the airfoil profile to be tailored to the transitory flight condition (Mach number, wing loading, etc.) over the entire mission. When a natural laminar flow (NLF) airfoil is forced to operate at a higher wing loading (higher lift coefficient) than it is designed for, the leading edge stagnation point moves further aft on the underside of the airfoil and a large suction peak is created as the flow accelerates around the leading edge. This ultimately results in a strong adverse pressure gradient over the forward part of the upper surface. This adverse pressure gradient forces the boundary layer to transition to turbulent – after which it grows significantly – often creating trailing edge separation. This separation is illustrated in the experimental data shown in Figure 4 (a) for an airfoil optimized for L/D at $C_L=1.0$ that is operated at $C_L=1.2$ ³. As mentioned earlier, a typical SensorCraft platform is expected to burn over half of its weight in fuel on a typical mission. The cruise-climb method of staying near the design lift coefficient is limited by engine specific fuel consumption per Mach and altitude and can be further constrained by sensor requirements. Figure 4 (b) illustrates the potential benefits of using variable geometry compliant structures to produce small, smooth deflections of the trailing edge of a Natural Laminar Flow (NLF) airfoil designed for a representative SensorCraft. Small deflections of the adaptive trailing edge are used to expand the laminar low-drag bucket by controlling the location of the stagnation point and hence the pressure gradient at off-design conditions. This enhanced capability will allow an entire mission to be performed at a reasonably high L/D .

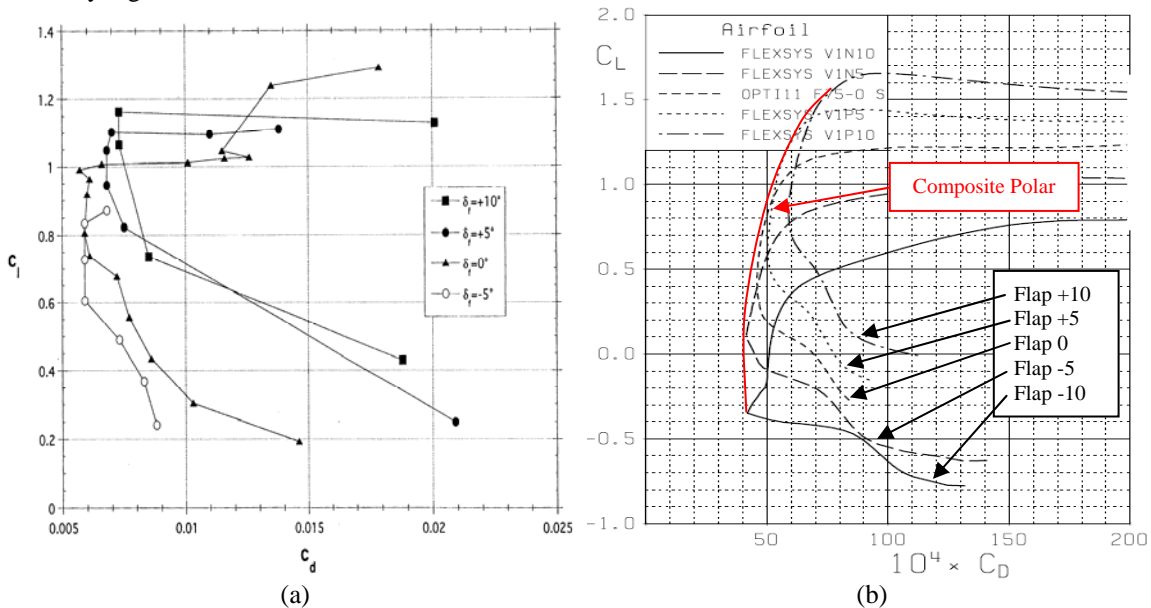


Figure 4. (a) C_L Vs. C_D experimental data for a modern long endurance airfoil with a conventional trailing edge flap³. (b) MSES generated plot showing the composite polar for a MAC-Wing flap airfoil.

II. Flight Test Model Description

The purpose of this test program is to quantify the aerodynamic and structural performance of a representative Mission Adaptive Compliant Wing (MAC-Wing) prototype system designed for high altitude, long endurance aircraft applications in relevant flight environments. The MAC-Wing prototype system was flight-tested using the Scaled Composite's White Knight aircraft, an aircraft that is capable of flying at altitude and Mach conditions compatible with long endurance aircraft conditions. The prototype model is designed for an aggressive, 65% chord, laminar boundary layer run on the upper surface that must be maintained over a range of operating lift coefficients using subtle MAC-Wing flap deflections. Relevant test conditions are best re-created in the low ambient turbulence, high altitude, flight test environment.

C. Model Description

The MAC-Wing model is shown in Figure 5. The wing has a 50 inches span and 30 inch chord (aspect ratio of 1.67). Elliptical endplates (45" x 24") help bound the flow and reduce three-dimensional effects. The wing is mounted in a cantilever arrangement with all loads channeled through one primary mount (at the bottom of Figure 5). The wing is capable of generating significant force; however, testing was limited to a maximum CL of 1.2 (roughly 950 lb of lift at flight test condition of 83 psf).

From 70% to 100% of the model chord is a structurally optimized variable camber flap driven by two electrical servo motors embedded inside the flap. The flap is capable of +/-10 degree change in camber (flap deflection) at rates up to 30 degrees per second (loaded). The upper surface of the flap consists of a smooth, continuous surface of an aluminum and polymer composition. The lower surface uses the same composition; however, an additional composite-reinforced panel is added extending from roughly 65% to 75% of the model chord. This panel allows the lower surface to expand and contract during flap deflection.

The leading edge of the flight test model is directly machined from 7075-T6 aluminum and holds tolerances as tight as +/- 0.0005" within the first 5% of the model chord. The surface of the model leading edge was ground to a 6 mil surface finish. The model incorporates an angle of attack servo system and a swing arm wake rake servo system. The aluminum leading edge is directly bolted to a heavy duty turntable bearing that securely fastens the wing to a fixed steel mounting plate. A linear actuator and pivot arrangement, located 15" radially from the turntable bearing center, controls the model angle of attack. A separate servo motor rotates the wake arm to sweep through the airfoil wake region (sweeps across the airfoil height).

With the exception of the compliant trailing edge flap, all structural components maintain safety factors of 8 or greater. The compliant trailing edge flap, due to its need to elastically strain, maintains a static loading safety factor of 2; however, the safety factor with respect to fatigue cyclic loading of this component is considerable (greater than 50).

The MAC-Wing model was mounted from the vertical stub pylon located on the underbelly of the Scaled Composites White Knight. Figure 6 shows the White Knight with the MAC-Wing model. During take off and landing, the ground clearance from the air data boom of the MAC-Wing model to the ground is 20 inches with the tires flat and the landing gear struts fully compressed.



Figure 5: MAC-Wing model was tested at the Subsonic Aerodynamic Research Lab at the Wright Patterson Air Force Base (June 2006) prior to the

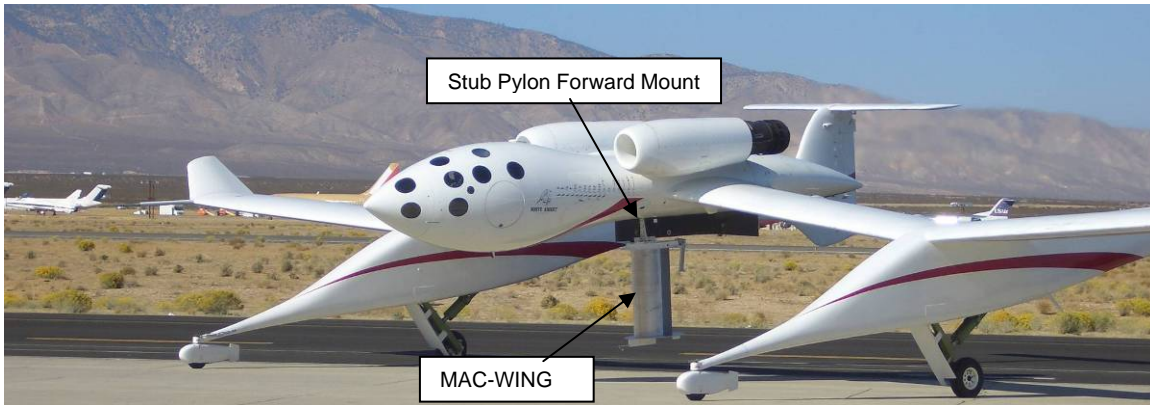


Figure 6. MAC-Wing mounted to Scaled Composites' White Knight Aircraft.

D. Instrumentation

The following items represent a brief description of all of the major systems that control, sense, acquire, and store information in the MAC-Wing model. Figure 8 shows a schematic of the model data acquisition and control system.

1. *Data acquisition system and model control interface.* A laptop computer serves as the central nervous system to monitor pressures, wake data, hot film data, as well as control angle of attack, the wake rake, and the compliant trailing edge flap servo systems. This computer is programmed using Labview and automates many of the data acquisition processes. Two National Instruments 16-bit, 200 kS/sec USB DAQ boards serve as principle data measurement modules. An RS485 card and cables connects all servo motors to the laptop. Figure 7 shows a screenshot of the data acquisition and control interface.

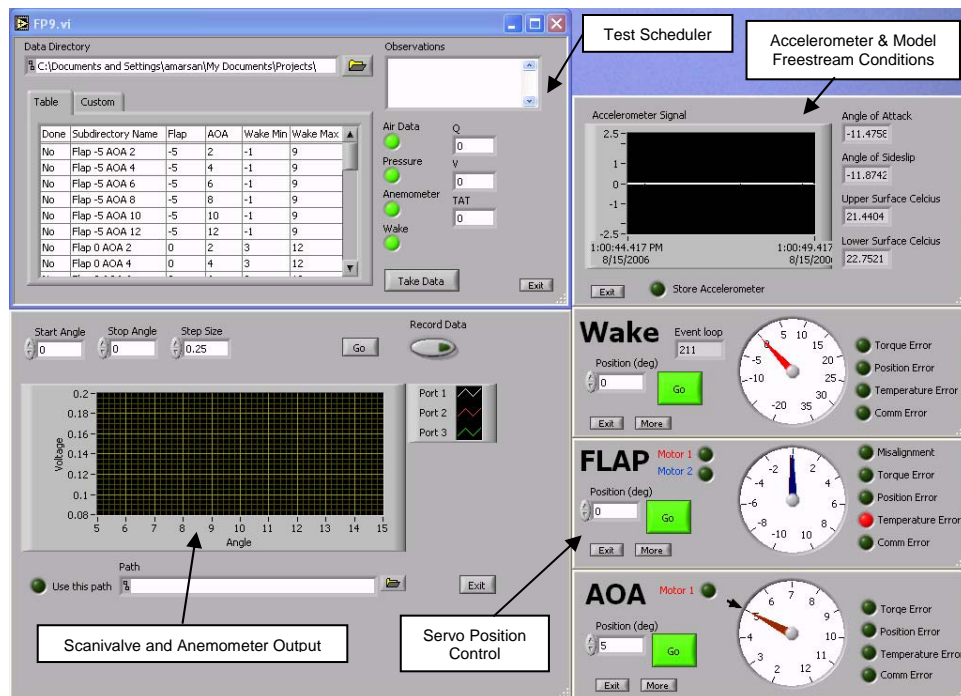


Figure 7. Screenshot of the data acquisition and model control interface.

2. *Pressure scanners.* One 64 channel and one 32 channel Scanivalve ZOC pressure scanning modules (www.scanivalve.com) are located in the outboard section of the model. A total of 76 0.040" diameter pressure taps – staggered at 15 degrees to prevent upstream laminar flow contamination – are used to record pressure over the surface of the airfoil. Other pressure sensor ports are used to instrument the

wake rake and the air data boom. Reference pressure is fed to the pressure scanners from the total pressure port on the air data boom which is read using an Omega absolute pressure transducer. In addition, information is logged from the White Knight flight computer.

3. *Model (geometric) angle of attack servo system.* A heavy duty turntable bearing is located at 23% chord and rigidly connects the airfoil to the mount plate. This bearing allows AOA rotation while sustaining shear and moment loads due to wing lift. A servo motor is mounted to the fixed mount plate. Using a 50:1 gearhead reduction combined with a ball screw drive system and pivoting mounts, the AOA unit is capable of rotating the model from +2 degrees to +12 degrees angle of attack. Hard stops are built into the unit to prevent further rotation.
4. *Swing arm wake probe.* A wake probe with two total and one static pressure probes were used to measure wake pressure profiles at all pertinent test conditions. This unit is mounted to the inboard elliptical end plate. The swing arm probe can traverse +/- 45 degrees to measure the airfoil momentum deficit.
5. *Hot film sensors.* Fifteen total Dantec Dynamics hot film sensors (www.dantec.co.uk) are arranged to measure the boundary layer transition position. These sensors are mounted on the airfoil upper surface at 24%, 34%, 43%, 48%, 53%, 58%, 63%, 66% and 68% chord position. In addition, hot films were mounted on the lower surface at 24%, 34%, 43%, 48%, 53%, and 58% chord position. Hot film sensors were read using a Dantec Dynamics 8 channel thermal anemometer which is capable of reading frequencies up to 10k Hz.
6. *Air data boom.* An air data boom from Space Age Control (www.spaceagecontrol.com) was mounted off the outboard elliptical end plate. This unit measured static pressure, total pressure, angle-of-attack and angle-of-sideslip information.
7. *Video cameras.* Three remote head video cameras were mounted to the inboard elliptical end plate to view the leading edge, the upper surface of the TE flap and the lower surface of the TE flap. A four-channel digital video recorder with an LCD monitor was used to view and record the model during all test procedures.
8. *Accelerometer.* An accelerometer is located at the outboard section at 65% chord to monitor model vibrations during flight testing.
9. *Model power supply system.* A series of DC to DC converters were used to step up or step down DC power from the aircraft 28 VDC bus supply. This power supply system was designed to provide minimal noise for signal-sensitive instrumentation while providing enough power for servo systems.

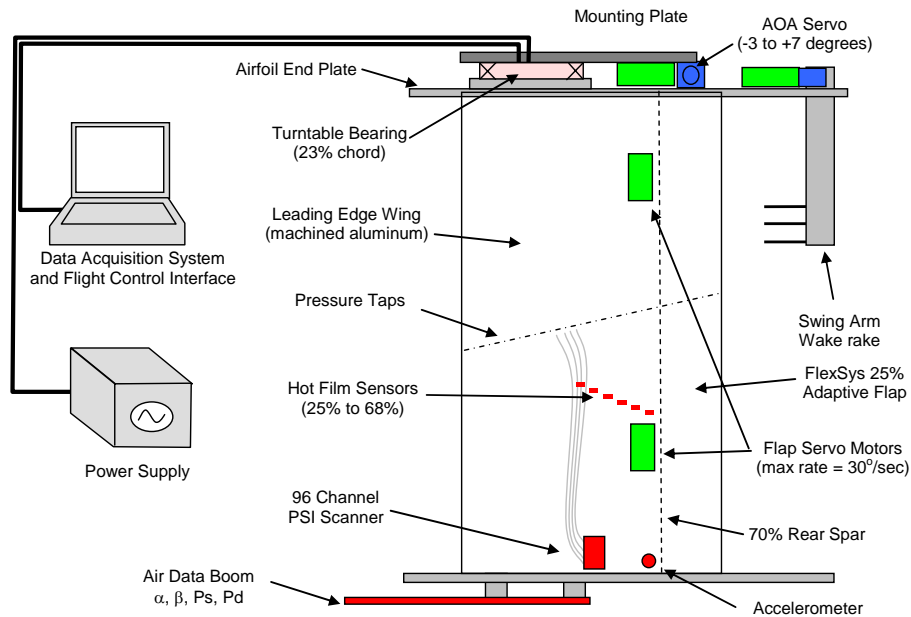


Figure 8. Data Acquisition and Model Control System.

III. Flight Test Method

Flight test was conducted at Scaled Composites facility at the Mojave civilian airport, Mojave, CA. The model was mounted to the underbelly of the White Knight stub pylon's forward fuselage attach point. The aircraft geometry forward of the test section provided a very clean aerodynamic environment with little disturbance of incoming air flow. The White Knight is powered by two Pratt and Whitney J-85 engines with afterburner. Thrust capabilities of these engines at high altitude allowed testing at velocities up to Mach 0.55 at 40,000 ft. This test point was the model's target Mach at the lowest possible altitude within the White Knight's flight envelope. Prior to testing, concern was expressed that the acoustic levels of these engines (even without afterburner) could interfere with laminar flow; however, test results proved this not to be the case.

Before attaching the model to the White Knight's pylon, all cables were routed into the fuselage through an access port in the stub pylon. After the installation of the model was complete, power and instrumentation components were secured inside the airplane's aft fuselage section. The data acquisition laptop and the video DVR were secured to the third seat in the forward cockpit for access by the co-pilot. All systems were then taken through ground testing and evaluation prior to first flight.

Test flights were performed over the Isabella MOA airspace. Flight testing was conducted at two primary test points: Mach 0.40 at 25,000 ft and Mach 0.55 at 40,000 ft – with the Mach 0.55 case being the primary case of interest. The Reynolds number at the 25,000 ft test point was 3.3 million; the Reynolds number at the 40,000 ft test point was 2.8 million.

Flight test procedures were strictly followed for safety and quality of data. Prior to flight, all model sensor and data acquisition and servo controls were given a thorough systems check and the model was wiped down – paying careful attention to clean any bugs or debris off the leading edge. After the model cleared this check, the aircraft was given a green light to fly. A pre-flight test meeting was held to discuss the model testing, aircraft altitude, Mach, and flight patterns to occur that flight. The aircraft was then rolled out of the hangar and prepped for flight. A two-man crew served to fly the aircraft and operate the MAC-Wing system. With the aircraft ready, both engines were started and the model power was switched over to the main generator bus. A final servo check was performed and a “begin flight zero-reference” data point was collected (gathering all sensor data) prior to take-off. At the end of each flight, an “end flight zero-reference” was also taken to look for any sensor drift over the course of testing. Also at the end of each flight, the model leading edge was thoroughly inspected for bug strikes and a post flight model systems check was performed.

The flight test plan consisted of envelope expansion, natural laminar flow testing and high rate flap demonstration. During envelope expansion, the stability and handling qualities of the White Knight were evaluated at various Mach and altitude test points. At each altitude, the pilot performed a series of maneuvers including stick raps at increasing speed, steady heading sideslips with the wing re-configured to its maximum lift setting and its minimum lift setting, and finally a 2.5 G pull-up maneuver.

After the model handling qualities were cleared at all altitudes and speeds, Natural Laminar Flow testing was conducted. The natural laminar flow test matrix consisted of 36 test points designed to measure the model lift, drag and pitching moment. Due to the model's finite aspect ratio, the test angle of attack of the model was significantly elevated over the infinite span CFD predictions. This led to rather high model angle of attack positions to push the lift range into the desired $CL = 0.4$ to 1.1 test range. Table 1 shows the NLF test matrix for the 40,000 ft test altitude. The data acquisition and control system software allowed the test point scheduler to automatically load the next test point in sequence. This procedure permitted testing to proceed at a rapid pace.

Table 1. AOA and flap deflections for the NLF test matrix.

<i>NLF Test Matrix for Test Point A (Mach 0.55 @ 40k ft)</i>					
<i>Lift and Moment Forces</i>					
AOA (deg) range	Flap (deg)	Estimated CL range	Estimated Lift (lb) range	Estimated CM range	Estimated Pitching Moment (ft-lb) range
2, 4, 6, 8, 10, 12	-5.0	0.11 to 0.92	130 to 714	0.02 to -0.003	37 to -6
2, 4, 6, 8, 10, 12	0	0.36 to 1.16	284 to 902	-0.06 to -0.08	-119 to -148
2, 4, 6, 8, 10, 12	+2.5	0.47 to 1.21	364 to 945	-0.10 to -0.11	-187 to -215
2, 4, 6, 8, 9, 10	+5.0	0.57 to 1.19	448 to 932	-0.13 to -0.15	-254 to -282
2, 4, 6, 7, 8, 9	+7.5	0.68 to 1.19	530 to 931	-0.17 to -0.18	-333 to -354
2, 4, 5, 6, 7, 8	+10.0	0.76 to 1.18	592 to 917	-0.21 to -0.22	-412 to -426

IV. Flight Test Results

Flight testing occurred during the months of October 2006 and December 2006. The weather in Mojave, CA was very good over the course of testing and there was rarely a day where testing could not be performed due to weather related issues. In some cases, an altitude had to be modified to move away from cloud layers in order to keep ice crystals from forming on the leading edge. By working with Scaled pilots, a sideslip tolerance of +/- 1 degree (which was AOA for the model) and a velocity tolerance of +/- 2 knots was established. In smooth air, these tolerances were held to tighter levels. Turbulence, however, made holding steady conditions more challenging. The onboard data acquisition systems on the White Knight and the MAC-Wing model allowed speed, altitude, and sideslip variability to be monitored. Bug strikes on the leading edge were practically nonexistent – only three bug strikes were observed on the leading edge during the entire 27 hours of flight testing.

E. Model Surface Pressures

Figure 9 and Figure 10 show the model surface pressures at the Mach 0.55 case at 40,000 ft. In Figure 9, the angle of attack is held constant and the flap is deflected to increase the lift generation of the wing. As the flap is deflected, the wing produces more and more lift; however, the pressure gradient on the upper surface over the first 60% of the model chord remains favorable thus keeping the boundary layer laminar.

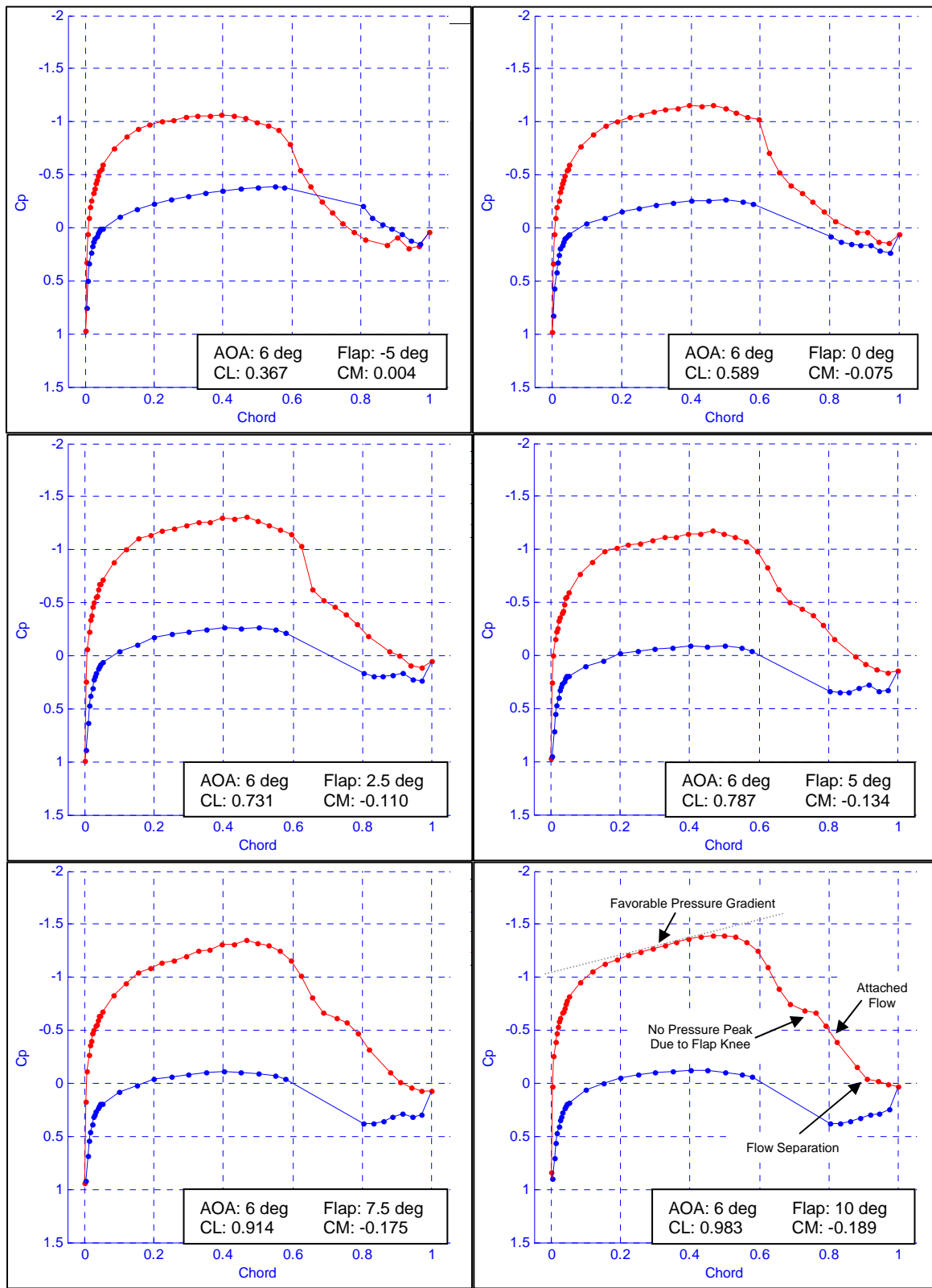


Figure 9. C_p distribution for constant AOA and changing flap deflection.

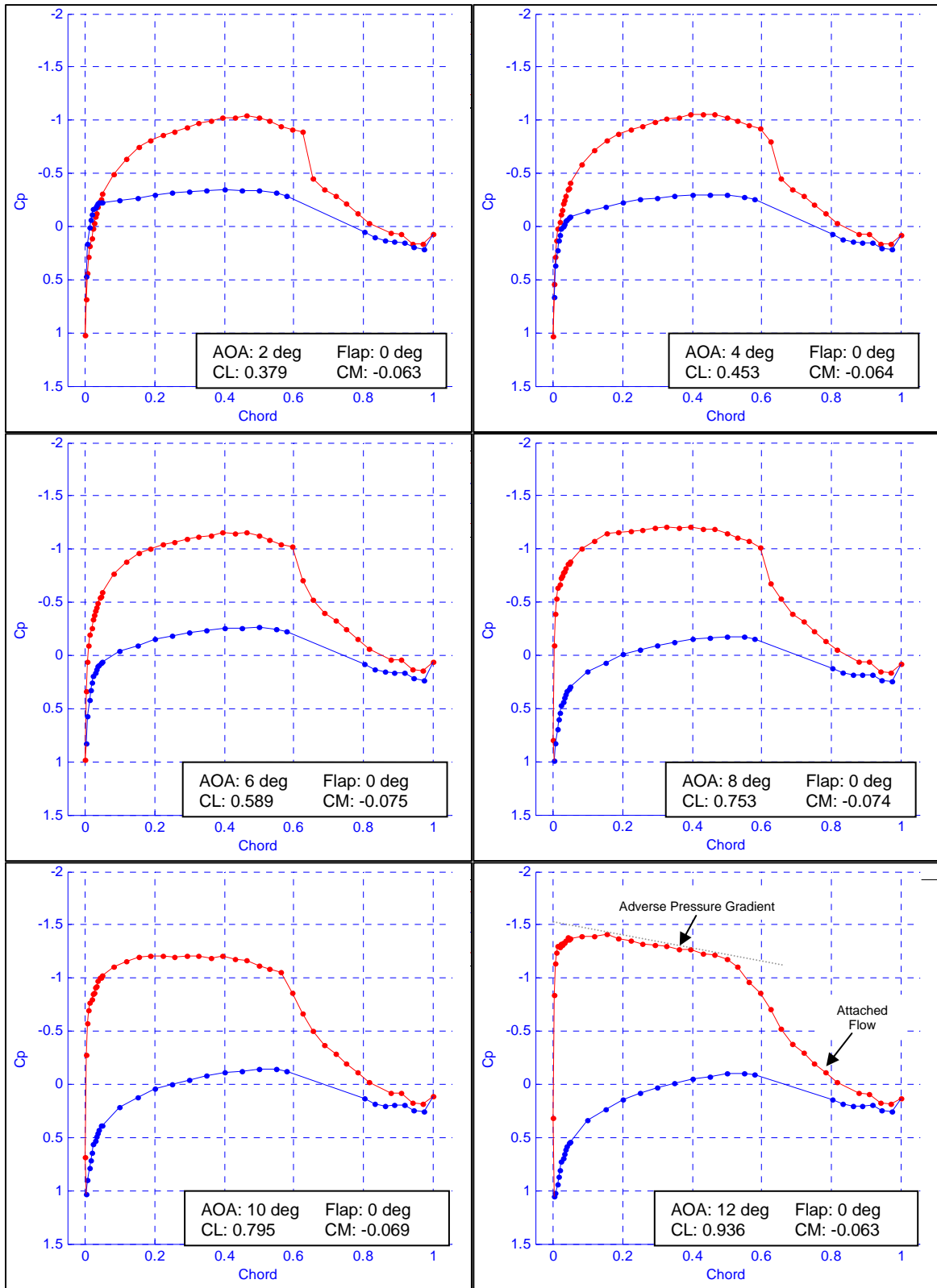


Figure 10. C_p distribution with flap fixed at 0 degrees and AOA varied to change lift levels.

At roughly 60% model chord, the airfoil geometry contains a subtle bump in the upper surface geometry to trip the boundary layer – as a turbulent boundary layer is more energetic than a laminar boundary layer and can maintain

attachment to near the trailing edge surface working against adverse pressure gradients. The steepness of the adverse pressure gradient in this model necessitates a smooth, variable geometry surface to maintain flow attachment – even when flap deflections are small.

In contrast to the case where the AOA is held constant and the flap is deflected, Figure 10 displays the CP curves as the flap is held constant and the AOA is increased to vary the lift production. The first 3 angles of attack from 2 degrees to 6 degrees maintain a favorable pressure gradient on the upper surface. The CP curve for the angle of attack of 8 degrees and 10 degrees maintain a marginal pressure gradient on the upper surface. The CP curve for the angle of attack of 12 degrees, required to achieve a lift coefficient of 0.936 has an adverse pressure gradient after the leading edge suction peak – promoting turbulent transition of the boundary layer.

F. Model Hot-Film Data

Hot film data was primarily tracked for the model upper surface. Hot films heat a very thin nickel resistive element deposited on a Kapton film to 100 to 150 degrees Celsius. A constant probe temperature is maintained by using carefully derived probe resistance measurements and a measure of the probe’s change in resistance per ΔT . Feedback control is performed by the Constant Temperature Anemometer (CTA) which can track up to 8 separate probes simultaneously (each probe has a separate resistance and percent resistivity measurement). A laminar boundary layer (versus a turbulent boundary layer) has a lower rate of convection and a much lower velocity variance. These physical differences show up as changes in the voltage signal output from the CTA (voltage signal is proportional to the probe current).

Hot film data was gathered at 1000 Hz for 8 seconds for each of the 8 films on the upper surface. By comparing a film’s voltage amplitude for a “zero White Knight velocity” condition and a “turbulent reference condition” (generated by placing a 0.005” trip strip on the model 5% chord and flying the model at several representative test points), we can qualitatively determine whether the boundary layer is laminar or turbulent. Note that a boundary layer does not instantly transition from laminar to turbulent and there are typically intermittency regions where the boundary layer is not consistently laminar or turbulent. Those regions are identified by bursting between a laminar signal and a turbulent signal.

Hot film data signals are plotted in Figure 11 for the case of 0 degree flap and 6 degree AOA ($CL = 0.589$), Figure 12 for 0 degree flap deflection and 12 degree AOA ($CL = 0.936$) and Figure 13 for 10 degree flap deflection and 6 degree AOA ($CL = 0.983$). Note that the average value of each signal is shifted to avoid overlapping voltage signals. The lower Reynolds number associated with flight testing at 40,000 ft provided a relatively resilient boundary layer and laminar runs could be achieved even with fairly unfavorable pressure gradients.

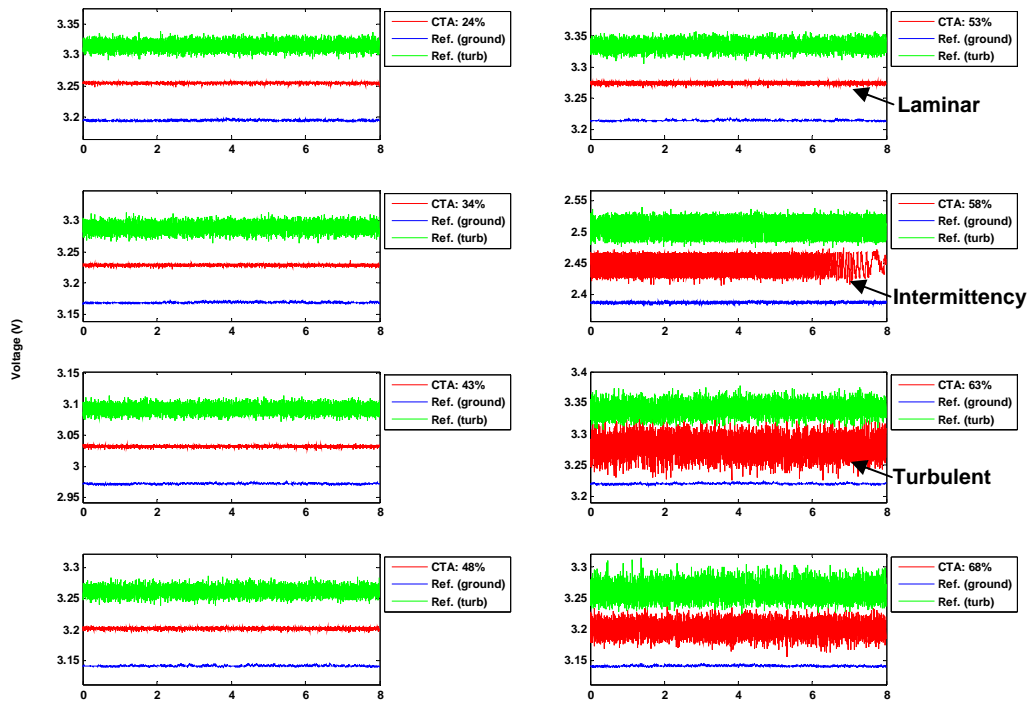


Figure 11. Hot film signals for 0 degree flap deflection and 6 degree AOA.

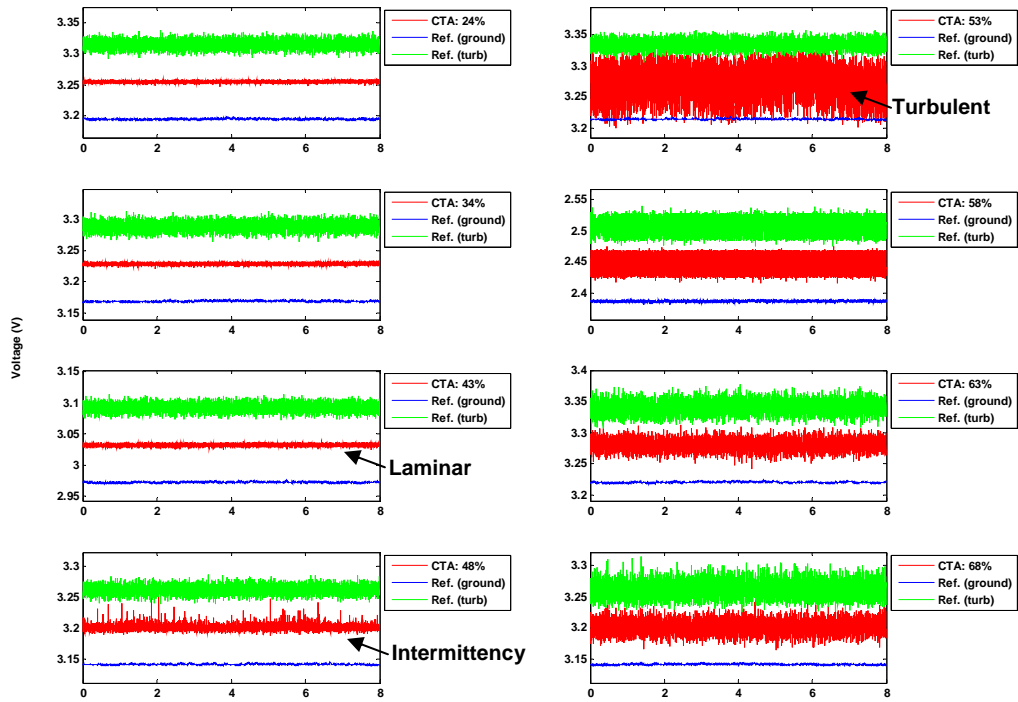


Figure 12. Hot film signals for 0 degree flap deflection and 12 degree AOA.

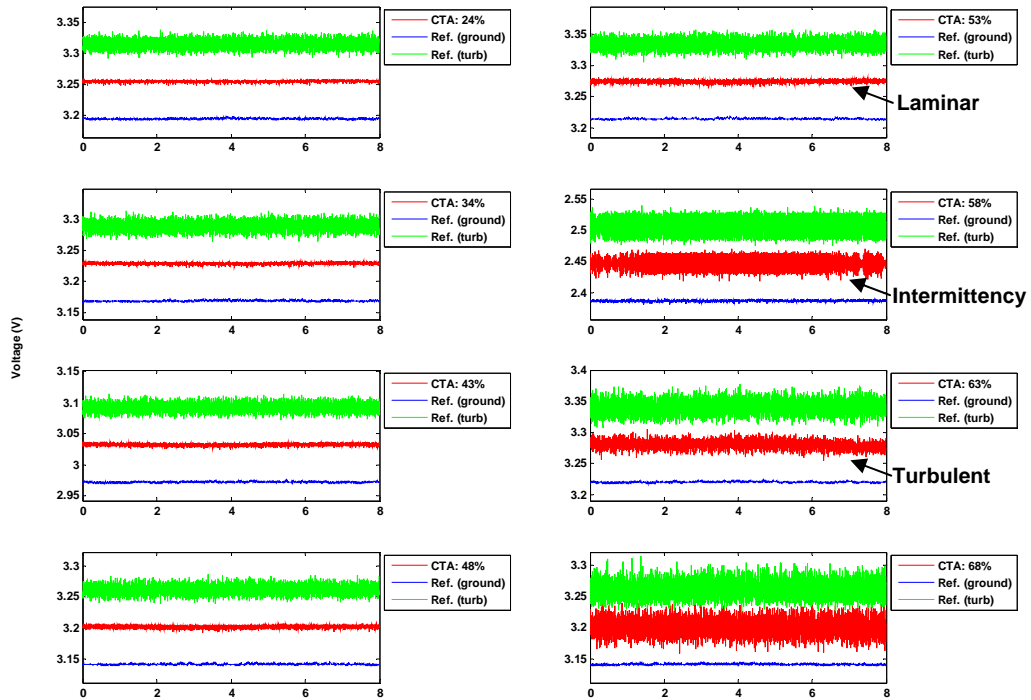


Figure 13. Hot film signals for +10 degree flap deflection and 6 degree AOA.

Figure 11 shows a typical case with the boundary layer remaining laminar through 53% chord. At 58% chord, the boundary layer is primarily turbulent but with a sharp drop in signal amplitude near the end of the 8 seconds which signals an intermittency region. At 63% of the chord and beyond, the boundary layer is consistently

turbulent. For the case of 0 degree flap and 12 degree AOA, Figure 12 shows laminar flow through 43% chord, the intermittency region beginning at 48% chord, and the turbulent region occurring at 53% chord.

In contrast, the hot film plot in Figure 13 with the flap at 10 degrees and the AOA at 6 degrees shows the intermittency region beginning at 58% chord and becoming fully turbulent at 63% chord. Thus even at these higher lift levels, laminar flow is maintained for roughly 10% longer using the compliant flap to generate lift rather than using the model angle of attack. Operation of the model at higher Reynolds numbers would likely make this incremental change in laminar flow chord percentage significantly larger.

G. Model Experimental Aerodynamics

Data is plotted for the model lift versus angle of attack (Figure 14) and pitching moment versus angle of attack (Figure 15), and finally for preliminary model lift to drag behavior (Figure 16). This data is compared to MSES⁴ two-dimensional, infinite span results for a wing at the same Mach 0.55, RN = 2.8 million conditions. The largest discrepancy occurs as the lift-curve slope is significantly different than an infinite span prediction. The reason for these discrepancies is due to the finite aspect ratio of the model. With no endplates, the model maintains an aspect ratio of 1.67; however, the elliptical endplates increase this aspect ratio. Using Equation 1⁵ we compute our model's aspect ratio to be 4.45. Thus, the elliptical endplates improve the wing's aspect ratio from 1.67 to 4.45. Larger endplates would have lessened the aspect ratio effect; however, the drag of the model would have increased to the point where the Mach 0.55 speed was not achievable.

$$\alpha' = \alpha + \frac{C_L}{\pi A} \quad (1).$$

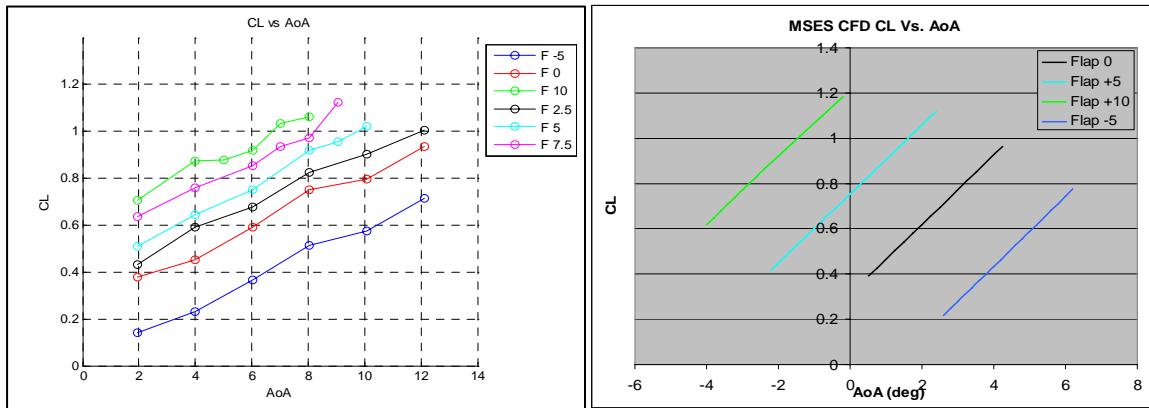


Figure 14. C_L Vs. AOA experimental data for the varying flap deflections compared to MSES 2D CFD predictions.

The aspect ratio also decreases the effectiveness of the flap. For the MSES case, a flap deflection of 5 degrees produces an offset in CL of 0.088 per degree flap deflection. The experimental data revealed an offset in CL that measured 0.036 per degree flap deflection. Thus, the finite aspect ratio behavior also affects flap effectiveness.

Moment predictions as compared to MSES 2D CFD are also displayed below. The primary shift in moment production occurs over a much broader angle of attack range. The magnitude of the moment production per flap deflection is largely unaffected by aspect ratio and pitching moment measurements agree relatively well with MSES predictions. Deflecting the flap does, however, produce a significant pitching moment. In practice, this pitching moment would be counteracted by correctly trimming the aircraft.

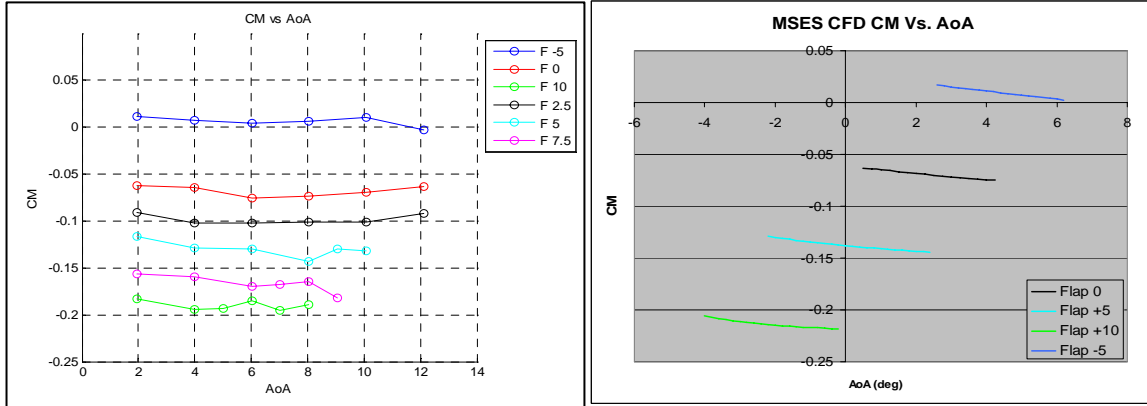


Figure 15. C_M Vs. AOA experimental data for the varying flap deflections compared to MSES 2D CFD predictions.

Drag measurements during flight testing are accomplished by sweeping pitot probes (total and static pressure probes) behind the model to survey the momentum deficit. The rotating arm wake rake was favored over a rake fixed to the trailing edge flap due to the ability of the wake to “curl” as a function of model flap deflection and angle of attack.

Currently, drag measurements are indicated as preliminary measurements. The goal of creating a C_L - C_D plot is to compute an equivalent two-dimensional lift and drag measurement from the MAC-Wing test results. This allows validation of the airfoil design procedure and the flap performance relative to the MSES CFD tool. Two-dimensional polar extraction is complicated by aerodynamic interference effects arising from the White Knight fuselage and wing. In addition, the low aspect ratio of the model produces three-dimensional effect which must be reduced. Extraction of a meaningful C_L - C_D polar will be accomplished in the near future.

Preliminary drag levels are calculated using Jones’ form of the drag equation which accounts for the non-zero static pressure field behind the model; however, currently p_2 is taken to be p_∞ for preliminary drag plotting purposes. The drag equation⁶ is shown below:

$$c_D = 2 \int_{-\infty}^{+\infty} \frac{g_2 - p_2}{q_\infty} \left(1 - \sqrt{\frac{g_2 - p_\infty}{q_\infty}} \right) d\left(\frac{y}{l}\right) \quad (2).$$

Drag polars for the experimental and CFD results are also displayed in Figure 16 for the lift coefficient ranges explored during testing.

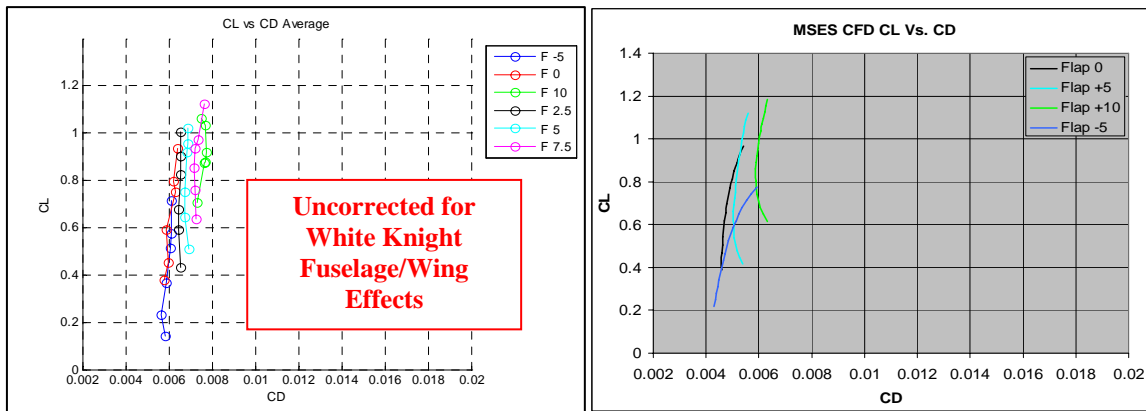


Figure 16. Experimental C_L Vs. C_D for varying flap deflections compared to MSES 2D CFD predictions.

Without corrections for White Knight interference and model three-dimensional effects, preliminary drag levels compare reasonably well with predicted MSES calculations. It is postulated that the correction to a two-dimensional C_L - C_D plot will lower the drag of the higher lift levels and broaden the low drag boundary of the wing’s

performance. Assuming that the final drag results compare favorably with the MSES projections, this opens the door for aggressive laminar flow airfoil designs at elevated Reynolds and Mach numbers. The resulting outcome will be that MAC-Wing technology and aggressive laminar flow airfoils can be applied to countless next generation high-performance, long-endurance aircraft.

H. High Rate Flap Testing

Because the MAC-Wing technology is primarily limited by the speed of the internal actuator (brushless DC servomotors in this embodiment), high flap deflection rates are achievable. The conclusion of testing involved a high rate demonstration at flap rates up to 30 degrees per second. These rates are compatible with performing Gust Load Alleviation (GLA) for SensorCraft vehicles to alleviate high moment loading (and high stresses) in the wing box. This GLA concept can allow for considerable weight to be pulled from the aircraft wing, allowing further gains in range and endurance. The following figures depict the wing at 25,000 ft Mach 0.4 moving at a maximum velocity of 30 degrees per second. The success of the high rate capability of the MAC-Wing model shows the great potential of this technology to impact SensorCraft and many other aircraft that can benefit from the variable geometry capability.

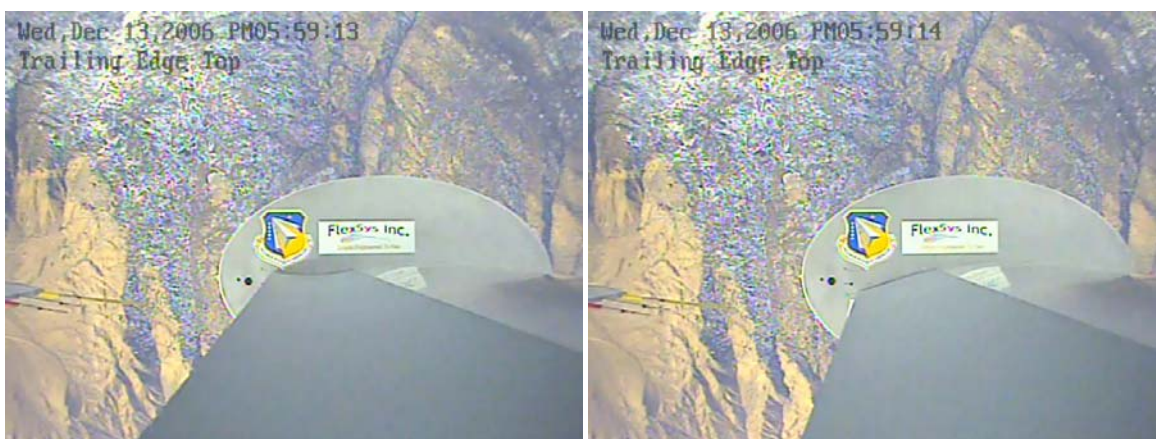


Figure 17. View from an in-board endplate camera showing trailing edge upper surface moving from -10 degrees to +10 degrees at 30 degrees per second.

V. Conclusions and Recommendations

The mission adaptive compliant flap can effectively control the upper surface pressure distribution while maintaining a sufficiently large transition radius into the pressure recovery region. This geometry minimizes flow separation and airfoil/wing drag. The aerodynamic data (lift, moment, and preliminary drag) measured during the flight test program agree reasonably well with the predicted levels determined computationally by AeroCraft using the MSES code⁴. The Dantec hot film sensor measurements on the wing upper surface confirmed extensive runs of laminar flow (up to 60% chord) even at high operating lift conditions. At higher Mach flight test point, $M = 0.55$, 40k ft., the test airfoil lift and moment levels tracked predicted level across the entire airfoil operating lift range. Drag data requires further processing in order to extract meaningful two-dimensional results from the described test set-up.

I. Endurance Aircraft Applications

The MAC-Wing flight validation experiment successfully demonstrated that an adaptive compliant trailing edge flap can be successfully designed, manufactured, and operated in an atmospheric environment compatible with long endurance military aircraft mission requirements. And, while it is difficult to determine the exact impact MAC-Wing technology might have on specific endurance aircraft without first knowing the configuration, prior Air Force sponsored studies² have shown that constant altitude endurance flight may be required to carry fuel loads of 45% to 55% of the aircraft gross weight. The ability to operate at minimum drag over large lift ranges is essential for fuel efficiency and mission success. Examining aerodynamic improvement alone, MAC-Wing technology has the potential for increasing the endurance of these air vehicles 15% or more. Therefore, MAC-Wing offers 15% or more in fuel savings. If gust load alleviation is taken into account or the ability of the flap to twist along the span to further lower wing root bending moment further, more dramatic weight savings are suitably envisioned.

Mission adaptive compliant wing technology has been brought to a technology readiness level that will support its application on the next generation high altitude long endurance aircraft. As demonstrated during the flight test program, the overall mission performance benefit of a carefully integrated variable camber trailing edge can be substantial. During flight testing, the MAC-Wing model was demonstrated at full scale dynamic pressure, Mach, and reduced scale Reynolds numbers. The flap was successfully operated in a high altitude, low temperature environment and did not encounter any operational restrictions or limitations. A final validation of MAC-Wing design/fabrication technology to consider might be actually replacing a trailing edge surface on a flying endurance aircraft with a compliant flap/control. A program of this type would demonstrate fully the aircraft structural integration aspects as well as highlight the lightweight and low power actuation benefits of MAC-Wing.

J. Transonic Cruise Aircraft Applications

With jet fuel prices high (if current trends are any indication heading higher in the foreseeable future) now is the time to aggressively pursue fuel savings technology on all fronts. FlexSys and others^{7,8} have studied the integration of a variable camber trailing edge to commercial transport aircraft for mission L/D optimization. Aerodynamic results from these studies were quite promising as indicated in Figure 18.

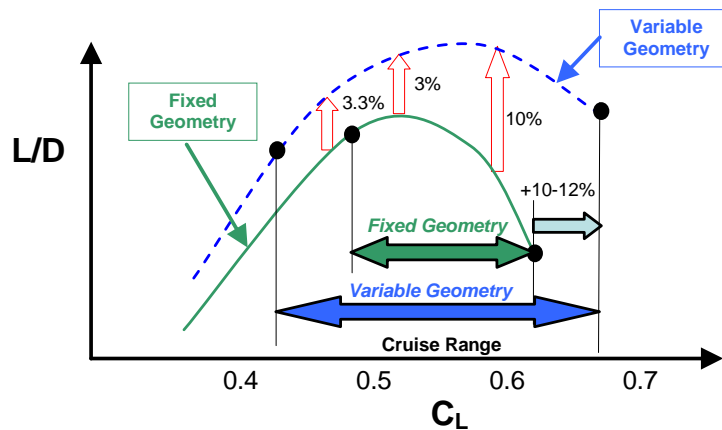


Figure 18. L/D improvement (Airbus A320) with variable geometry trailing edge.

These results⁷, appear to offer a substantial mission performance improvement (fuel savings); however, the variable geometry implementation proposed by Airbus required moving, and holding the high lift trailing edge flap during high “q” cruise conditions. The resulting weight penalty in the flap structure/actuation system reduced the estimated performance improvement by one half in the heart of the cruise performance envelope.

Taking a lead from the Northrop-Grumman study comparison of smart-Wing concepts for transonic cruise drag reduction⁸, FlexSys has conceptualized an integrated trailing edge that merges the variable camber into the aft element of the high lift flap as shown in Figure 19.

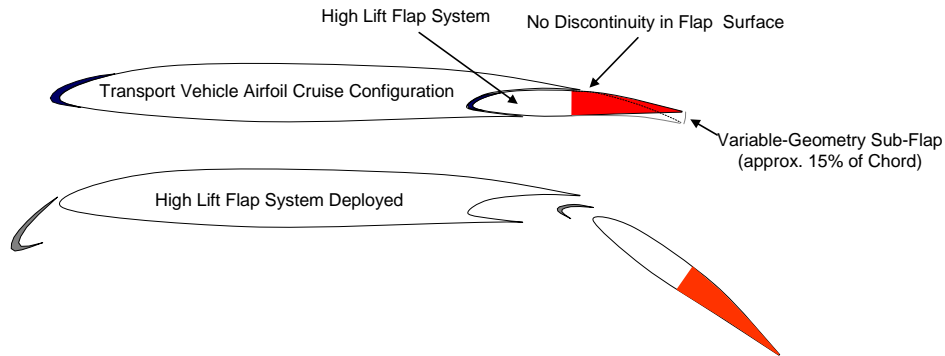


Figure 19. FlexSys high lift flap with cruise variable geometry feature.

The compliant structure, variable geometry addition to the aft flap element can provide camber control needed to produce performance levels similar to those presented in Figure 18. For example, a medium range transonic

transport incorporating the flap system shown is projected to save over 100 gallons of jet fuel on a cross country flight (compliant flap cruise L/D improved 3.3%). Depending on aircraft utilization, fuel savings of 64,000 gallons/yr per aircraft are anticipated. A 3% fuel saving with a retrofit MAC-Wing across the entire US aircraft fleet could save over \$1.2 billion per year based on current fuel costs. A new wing design that capitalizes on the capabilities of MAC-Wing could save as much as 15% in fuel costs plus additional gains from weight savings due to (a) less fuel (b) smaller wing-root-bending-moment, and (c) lighter (smaller chord) and more efficient flap.

The aerodynamic benefits of a smooth, variable camber flap are significant. Comparing a MAC-Wing flap to a conventional trailing edge flap during a max G pull-up maneuver showed that the MAC-Wing flap actually required 33% less actuation force and 17% lower peak actuation power. Comparing equally sized trailing edge flaps, MAC-Wing flaps can provide up to a 40% increase in control authority per degree deflection over hinged control surfaces.

A flight validation program to verify variable geometry cruise control performance enhancement on a transonic transport aircraft configuration would be beneficial to both future military and commercial aircraft development programs.

Acknowledgments

FlexSys Inc. is grateful for the support of Air Force Research Lab VAAA in funding this work. Their continued support has allowed significant and rapid maturation of the MAC-Wing technology. FlexSys would also like to thank Hal Youngren of AeroCraft for his tireless work and contribution to the program and to Lockheed Martin for their technical support and input to the model design. Finally, FlexSys would like to thank Scaled Composites for their time and talent in making this flight test a success and a thoroughly enjoyable experience.

References

¹Kota, S., Hetrick, J., Osborn, R., Paul, D., Pendleton, E., Flick, P. and Tilmann, C., "Design and Application of Compliant Mechanisms for Morphing Aircraft Structures," Paper 5054-03, *SPIE Smart Structures and Materials Conference on Industrial and Commercial Applications of Smart Structures Technologies*, San Diego CA, 2-6 March 2003.

²Tilmann C.P., Flick P.M., Martin C.A., Love, M. H., "High Altitude Long Endurance Technologies for SensorCraft", *RTO AVT Symposium on "Novel Vehicle Concepts and Emerging Vehicle Technologies"*, Brussels, Belgium, 7-10 April 2003. Published as RTO-MP-104.

³Reed, S.A., "High Altitude Long Endurance Airfoil Performance Validation", WL-TR-96-3091, Flight Dynamics Directorate, Wright Laboratory, Wright-Patterson AFB, OH, January 1996.

⁴Giles, M. B., and Drela, M., "Two-Dimensional Transonic Aerodynamic Design Method," *AIAA Journal*, Vol. 25, No. 9, 1987, pp. 1199-1206.

⁵I. H., and von Doenhoff, A. E., *Theory of Wing Sections*, Dover, New York, 1959.

⁶Schlichting, H. and Gersten, K., *Boundary Layer Theory*, Eighth Edition, Springer, Berlin, 2000.

⁷Greff, E., "The Development and Design Integration of a Variable Camber Wing for Long/Medium Range Aircraft", *Aeronautical Journal*, November 1990.

⁸Austin, F., Siclari, M. J., Van Nostrand, W., Kottamasu, V. and Volpe, G., "Comparison of Smart-Wing Concepts for Transonic Cruise Drag Reduction", *SPIE Smart Structures and Materials Conference*, San Diego, CA, 4-6 March 1997.